

Exoplanet Transit Observation using a Digital Single Lens Reflex Camera in an Urban Setting

Philippe Joly

Vanier Cégep/College, Montréal, Quebec, H4L 3X9, Canada
2151940@edu.vaniercollege.qc.ca

Submitted: May 19th, 2023

Abstract

The advent of the new James Webb Telescope put a spotlight on astronomy and the search for new exoplanets. Beyond the JWST, a lot can be done without such expensive equipment, opening the field to a broader number of potential observers. Inexpensive consumer-grade DSLR cameras have already been shown to have the ability to observe exoplanet transits. This paper explores if these findings can be replicated in an urban light-polluted area. Following the American Association of Variable Star Observers' guide on DSLR photometry [9]. We attempted to observe the transit of exoplanets around HAT-P-20, HAT-P-22, and TOI-1131 using a *Canon Rebel T3i* DSLR camera and a 28000 mm focal length *Celestron Advanced VX* Schmidt-Cassegrain telescope at the Vanier College observatory in Montreal, Canada – where the sky's brightness can exceed 17 mag/arcsec² [17]. The data was extracted manually, performing aperture photometry using *Iris* [3]. The transit of HAT-P-22 April 2nd, 2023 was observed successfully, demonstrating the feasibility of observing a transit using a DSLR camera in a heavily light-polluted area such as Montreal. However, the observational data for HAT-P-20 and TOI-1131 is inconclusive, as no transit was observed during the observational periods – expected transit times. From the results and the properties of the three host stars, it is concluded that, under similar conditions, potential observable transiting target stars should be brighter than 10 mag with a transit depth larger than 0.01 mag. Furthermore, refining the observation process could enable systematic observation of transits and the extraction, modelling, and analysis of more precise transit data despite poor observational conditions and equipment.

1 Introduction

Over 5000 exoplanets have been discovered in our galaxy [1]. This is an exceptional feat of the scientific community as the first confirmed exoplanet dates back to the year 1992 [1]. Nevertheless, there are thousands more candidate stars around which potential exoplanets could orbit [1].

This relatively new field as well as the significant number of potential targets necessitates a great number of observations and observers. This incites a diversification of the observer body and encourages amateur and upcoming astronomers to get involved and to participate in this scientific effort. The broadening of the astronomical community creates a need for affordable astronomical equipment and techniques.

Researchers have experimented with digital single lens reflex (DSLR) cameras in replacement of charged-coupled device (CCD) cameras – their much

more expensive counterparts – and have found that they have the ability to produce meaningful photometry [11] [16] [27].

As DSLR cameras capture an image, the incoming light is converged on a complementary metal oxide semiconductor (CMOS) detector [9]. The CMOS detector is covered with a Bayer filter restricting the wavelengths hitting each pixel to a specific range [9]. With the Bayer filter, pixels of the CMOS detector capture light from either the red, blue, or green spectrum [9]. On the other hand, most CCD cameras do not have an inherent array filter, like the Bayer filter, capturing light monochromatically [19]. In a CMOS sensor, Pixels contain a photo-diode which, when hit by light, sends electric signals to a processor which converts the electron count to Analog Digital Units (ADU) stored in a digital image file [9].

In astronomy, CCD cameras are used over their DSLR counterparts as they offer better light sensitivity due to their inherent design which achieves

efficient light collection and low noise [19]. In fact, the noise [21] is further reduced as they are often cooled whereas the internal temperature of a DSLR camera can greatly vary throughout observations affecting the results and increasing the noise [9]. Nevertheless, DSLR cameras can be a good option for upcoming astronomers because of their low cost and how easy they are to work with [9].

John E. Hoot, in 2007, tested the efficiency of DSLR cameras in an astronomical context. Making observations of Landolt standard star fields using a *Canon EOS 350D* DSLR camera [11]. Hoot concluded that DSLR cameras have a limited observational span of less than 2.5 mag [11]. Nevertheless, he asserts that DSLR cameras are suitable for multi-band (*i.e.* on all three colour channels) differential photometry which happens on the scale of milli-magnitudes [11]. In other terms, Hoot determines that DSLR cameras can perform accurate differential photometry such as observing an exoplanet transit as long as comparison stars are within that range of 2.5 mag [11].

In 2010, Colin Littlefield – a member of the Department of Physics of the University of Notre Dame – was successful in observing the transit of the exoplanet HD 189733b of apparent magnitude 7.67 mag with a depth of 0.028 mag using a *Canon EOS 20Da* DSLR and an eight-inch Schmidt-Cassegrain *Celestron CPC 800* telescope [16]. Littlefield found that, in his observations, the green channel showed the best signal to noise ratio [21] as it is an average of two channels with the highest sensitivity, whereas the red one showed the worst [16]. Littlefield attributes the red channel's low signal to noise ratio to DSLR cameras' infrared blocking filter, which also suppresses low-frequency light [16].

In a different approach, M. Zhang *et al.* from Princeton investigated the precision of DSLR photometry combining the three color channels [27]. They integrated a *Canon EOS 60D* DSLR camera to the *HATNet* sky survey and compared the data of 6600 stars made with the DSLR camera with the data acquired with an industry-standard CCD camera [27]. They found through statistical analysis that the *Canon EOS 60D* DSLR camera are a capable observation tool reaching a median absolute deviation of 4.6 mmag combining all channels with a 180 s exposure time, which would make the *Canon EOS 60D* capable of detecting transits of hot Jupiters [27]. As a proof of concept, Zhang *et al.* successfully observed the transit of the exoplanet KELT-3b using the *Canon EOS 60D* DSLR camera [27].

The proof of concept that DSLR cameras are viable instruments to perform meaningful astronomical photometry creates an affordable entry way to observational astronomy participating to innovation within the field. However, the reach of these findings is somewhat limited in the way these observations are conducted. Littlefield [16] and Zhang *et al.* [27] show the effectiveness of DSLR cameras in remote quasi-ideal observational locations. Locations with poor seeing and high levels of light pollution – often cities – are often avoided in astronomy as the overall bad observational conditions can significantly impact quality of the results and findings. The more severe the light pollution is, the brighter the sky gets, and the number of observable stars shrinks as they get fainter with respect to the bright sky. Nonetheless, being able to conduct useful DSLR photometry on variable stars in urban centers would allow an even greater number of amateur astronomers to participate to the expansion of our exoplanet catalogs.

This paper explores if a consumer-grade DSLR camera can perform precise and accurate photometry in an urban setting. More precisely, it is trying to determine the feasibility of observing an exoplanet transit in a city with poor observational conditions with a DSLR camera.

This research attempts to observe an exoplanet transit using an eleven-inch aperture Schmidt-Cassegrain *Celestron Advanced VX* telescope with a focal length of 28000 mm along with *Canon Rebel T3i* DSLR camera in the Vanier College observatory situated in Montreal, Quebec, Canada, where the sky's brightness can get up to $17.80\text{ mag/arcsec}^2$ [17].

2 Methods

Three different targets were observed at the Vanier College observatory using a *Canon Rebel T3i* DSLR camera and a *Celestron Advanced VX 11"* Schmidt-Cassegrain telescope: HAT-P-20, HAT-P-22, and TOI-1131 on the nights of March 19th, April 2nd, and April 15th, 2023 respectively. The data was then reduced, treated, and analysed using the Iris software as well as Python. Most of the observational procedures such as the acquirement of calibration frames is taken from the The “AAVSO DSLR Observing Manual” [9].

2.1 Hardware and Camera Setup

The telescope used, the *Celestron Advanced VX*, is a Schmidt-Cassegrain telescope with an 11" aperture and a 2800 mm focal length. The telescope is mounted on a *Celestron CGX-L* german equatorial mount in the Vanier observatory. The Vanier dome is situated on the rooftop of Vanier College in Saint-Laurent, Montreal, Canada. More precisely, it is situated at latitude 45.52° and longitude -73.68° . In addition to the bright Montreal sky, Vanier College keeps its spotlights turned on all through the night resulting in a very bright observational environment.

The *Canon Rebel T3i* used is equipped with a 14-bit 22.3×14.9 mm CMOS sensor with 18 effective megapixels. Attached to the *Celestron Advanced VX*, its field of view is 27.38×18.29 arcmin. Canon's RAW image capture setting was used to make the observations. For the first observation (HAT-P-20), as we were still familiarizing ourselves with the camera, the white balance and Picture Style settings were left as Auto and a international organization for standardization (*i.e.* ISO) value of 100. For the two other observations, the Picture Style was set to Monochrome, the white balance was turned off, and the ISO was set to 800. On the third set of observation, the Auto Flip feature was also turned off. Some inherent features of the camera can not be altered such as the infrared filter blocking a portion the incoming low-frequency light as well as its automatic noise reduction feature which is applied for long-exposure shots [16].

2.2 Software

During this research, software were used to control the mount, capture images, and reduce the observations. The *Celestron PWI* [7] software was used to align and orient the mount on our targets ensuring tracking throughout the observations. The *EOS Utility 4.0* [5] along the *Canon Digital Photo Professional* software [6], connected to the camera, were used to capture images with specific settings at given intervals automatically. The Iris software was used for image reduction and processing for its simplicity and ability to work with *Raw Canon* DSLR files (*i.e.* .CR2 files). Other important resources used in this research are the *SIMBAD Astronomical Database* [26] as well as the finding charts tool offered by Swarthmore College [13] to identify potential comparison stars in the field of view.

2.3 Calibration Frames

Calibration frames were taken during each observations. The flat fields were taken before sundown with a 25 second exposure time capturing a distant 27.38×18.29 arcmin section of the sky close to the zenith, which we assume to be evenly illuminated. The bias and dark frames were taken before, during, and after the observations by closing the telescope's aperture with its lid [9]. The bias frames were captured using the camera's lowest exposure time of $1/4000$ s whereas dark frames were taken with exposure times equivalent to that of the scientific images. It goes without saying that all of these calibration frames were performed at the same ISO value as the scientific images.

2.4 Observations

Three sets of observations were attempted, each building on the mistakes and the improvements of the last.

2.4.1 Target Selection

When determining potential targets, the star's magnitude, the transit's depth, time, and duration, as well as the star's altitude during the transit were considered. To explore observable transits, we used the *Variable Star and Exoplanet Section of Czech Astronomical Society*'s website [20] which regroups information about an extensive number of known transiting variable stars. To maximize the chances of observing a transit, targets with the lowest magnitude as well as the highest transit depth and length were chosen [9]. We also aimed for transits at times around 22h00 to 2h00 at high altitudes to achieve a darker sky and to mitigate the affects of atmospheric turbulence.

2.4.2 HAT-P-20

The first target, HAT-P-20, has a magnitude of 11.34 mag. The transit we were trying to observe was recorded to have a depth of 0.0204 mag and a duration of 110.88 minutes [20]. TYC 1914-551-1 of magnitude 10.54 mag which is not a known variable star was used as a comparison star [26] [13]. The transit was set to happen on March 19th 2023 from 21h25 until 23h15 EDT starting at an altitude of 67° and ending at 52° [20]. We started observations of the target at approximately 21h10 and stopped towards 23h30 EDT. The time of the observational images is uncertain as the date and time recorded in the image header was that of the camera, which was

incorrect, instead of that of the computer. This issue was fixed for the two following observations. The sky was mostly clear throughout the night with temperatures around -4.8°C [4]. The scientific images were taken with an exposure time of 120 seconds and an ISO of 100 at 10 second intervals.

2.4.3 HAT-P-22

HAT-P-22 has a magnitude of 9.73 mag and its transit was previously observed to have a duration of 172.2 minutes and a depth of 0.0140 mag [20]. It was predicted to start 22h40 EDT April 2nd 2023 at an altitude of 86° ending at 01h32 EDT the day after at 60° [20]. The chosen comparison star is HD 233728 has a magnitude of 9.39 mag and is not a known variable star [26] [13]. Our observations spanned from 22h15 EDT until 01h59 EDT at 10 second intervals. An ISO of 800 and an exposure time of 70 seconds were used for most of the scientific images. However, due to a human mistake, some of the scientific images have exposure times of 80 and 90 seconds. To account for this, dark frames of 70, 80, and 90 second exposure were used for calibration. The observational conditions started acceptable with temperatures hovering around -7.3°C [4] and with variable sky conditions.

2.4.4 TOI-1131

The last target, TOI-1131, has a magnitude of 9.7 mag . Its transit was previously observed to have a depth of 0.0043 mag and a duration of 42 minutes [20]. It was predicted to be observable from 23h09 until 23h51 EDT on April 15th 2023 with an altitude varying from 48° to 53° [20]. The chosen comparison star is TYC 4190-97-1, which is a star not known to be variable with a magnitude of 9.56 mag [26] [13]. Our observations started at 22h39 and ended at 00:19 with exposure times of 55 seconds, ISO values of 800, and 5 second intervals. The sky remained clear throughout the night with temperatures surrounding 6.6°C [4].

The fields of view from the observations of HTA-P-20, HAT-P-22, and TOI-1131 used for data processing and analysis can be seen in Appendix A.

2.5 Image Reduction and Photometry

The *Iris* software [3] was used for the treatment and analysis of scientific and calibration images. *Iris* was chosen for its ability to process and work with three channels *RAW* DSLR data. For the observations

of HAT-P-20 and TOI-1131, the stacking and creation of master calibration frames as well as the reduction of the scientific images was performed as described in the described AAVSO's *IRIS-Beginner Tutorial* [8]. The observations of HAT-P-22, on the other hand, were reduced, summing the three channels into one using the *Numpy* [10], *Rawpy* [23] and *Astropy* [2] modules [Appendix B] [22] and then following the same procedure as for the two other sets of observations.

Neither the plate solving nor the image alignment features of *Iris* could be used on the data as stars in the field of view were too few and dim. The significant movement of the field of view between exposures also participated in preventing any alignment tools on the scientific images. Hence, the stars' flux was measured manually using *Iris*' aperture photometry software [3]. The stars' full width half maxima (measured using *Iris*' point spread function tool [3]) were used as the inner aperture radii [Figure 1]. Those values doubled were used as the annulus' inner radius and the annulus' outer radius was chosen to be of 20 additional pixels [Figure 1]. Flux and median background values were recorded that way for the target and one comparison star across all scientific images for all three observations. A considerable portion of the scientific images are omitted as the stars are often too dim with respect to the background or their trail too pronounced.

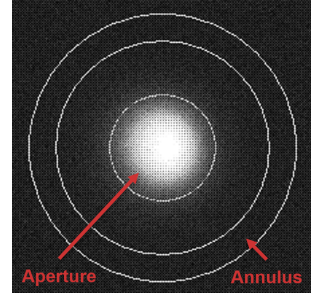


Figure 1: Aperture of HAT-P-22, with the Inner Circle and the Outer Ring respectively Delimiting the Star's Aperture and the Annulus

2.6 Data analysis

The extracted aperture photometry data was compiled as text file from the *Iris* output box. The data was extracted parsing through the text file [22]. Flux data from both the target and comparison stars were processed subtracting the product of the median background value and the number of pixels in the inner aperture. The light curves were obtained

by graphing ratio of the target’s adjusted flux with respect to that of the comparison star over time using the *Numpy* [10], *Rawpy* [23] and *Matplotlib* [12] modules [Appendix C] [22]. The uncertainty used is the noise derived from the roots of the target and comparison stars’ adjusted fluxes using the *Uncertainties* module [15]. The data was matched to the extracted time data from the CR2 file headers using *ExifRead* [24] [Appendix C] [22]. The data retrieved from the observation of HAT-P-22 was then combined doing a 5-point and 3-point average of normalized flux over time using the *Numpy* [10] module [Appendix D] [22]. Then, using the *Numpy* [10] and *SciPy* [25] modules, a best fit quartic curve was created to outline any variation in the target star’s normalized flux [Appendix D] [22].

3 Results

We were able to observe the transit of HAT-P-22 during the expected transit period on April 2nd, 2023 denoted by the reduction in the star’s relative flux in Figure 5. The reduction in relative flux of HAT-P-22 is further highlighted by combining data points in groups of 5 [Figure 6]. On the other hand, after observing HAT-P-20 and TOI-1131 during the predicted times of transit, we were not able to observe a significant drop in relative flux indicative a transit [Figure 2] [Figure 4].

As seen in Figure 2, a large portion of the data points during the observation period of HAT-P-20 had to be omitted from the analysis as the stars were often too dim with a brightness comparable to that of the sky. The light curve Figure 2 shows no dip in the relative flux of HAT-P-20 with respect to TYC 1914-551-1 across the observation. As a consequence, we can not observe the transit from the collected data as shown in Figure 2.

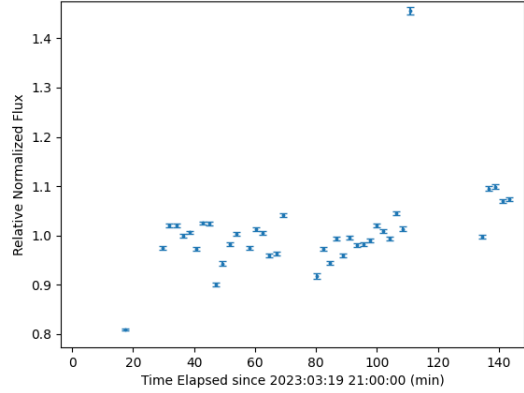


Figure 2: Relative Normalized Flux of HAT-P-20 on TYC 1914-551-1 on March 19th, 2023 from 21h10 until 23h30 EDT

Some scientific images from the TOI-1131 observation also had to be discarded because of the poor tracking. Although the weather conditions were good, the mount’s tracking was bad enough that the target star and TYC 4190-97-1 are stretch and have a significant trail in several of the scientific images as seen in Figure 3. From the usable data, we cannot arrive to the conclusion that a transit occurred as there is no apparent dip in the relative flux of TOI-1131 as seen in Figure 4.



Figure 3: Image of the Field of View of TOI-1131 on April 15th, 2023 at 22h54 and 25 Seconds EDT Showing the Trails Caused by Poor Mount Tracking

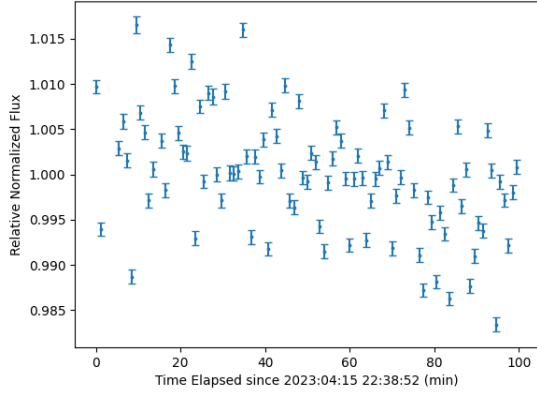


Figure 4: Relative Normalized Flux of TOI-1131 on TYC 4190-97-1 on April 15th, 2023 from 22h39 until 00h19 EDT

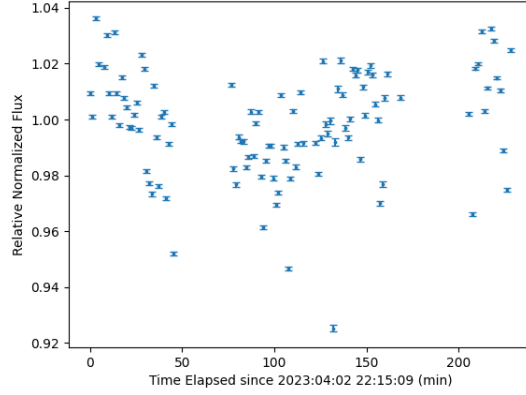
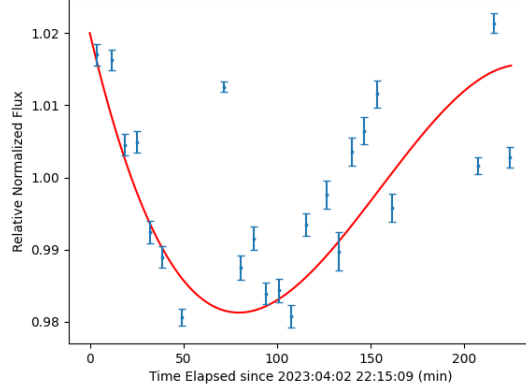


Figure 5: Relative Normalized Flux of HAT-P-22 on HD 233728 on April 2nd, 2023 from 22h15 until 01h59 EDT



Similarly, a considerable portion of the scientific images of HAT-P-22 had to be discarded as cloudiness formed around one hour and two hours in our observations, resulting in the target star and HD 233728 to be barely distinguishable from the background sky. Additionally, due to poor tracking, either the target or comparison stars were outside the field of view for some of the frames. Nevertheless, the HAT-P-22 light curve, outlining a dip in relative flux considerably more significant than the values' uncertainties, indicates a transit [Figure 5]. The reduction in relative flux is further illustrated combining data points – taking a 5-point average – and fitting a quartic curve to the combined data set [Figure 6] [Appendix D]. This process was also performed combining data points in groups of 3 [Figure 10], resulting in the same conclusion that a transit of HAT-P-22 occurred during the observation.

Figure 6: Relative Normalized Flux of HAT-P-22 on HD 233728 on April 2nd, 2023 from 22h15 until 01h59 EDT, with Combined Data Points (a 5-Point Average) and Transit Outline

4 Discussion and Conclusions

This research project explored the feasibility of performing meaningful photometry using a DSLR camera in an urban setting by trying to observe a transit. Using a *Canon Rebel T3i* and a *Celestron Advanced VX* Schmidt-Cassegrain telescope, the transit of HAT-P-22 was observed on April 2nd, 2023, during expected transit times [Figure 5] [Figure 6]. This transit observation exhibits DSLR cameras' photometric potential even in poor observational condi-

tions. However, HAT-P-22 was the only observed transit among three observations during predicted transit times, as there is no significant drop in relative flux indicating a transit in the light curves of HAT-P-20 and TOI-1131 [Figure 2] [Figure 4]. We can conclude that it is feasible to record a exoplanet transit using a consumer-grade DSLR camera in an urban environment, depending on the transit and host star's properties.

The high variability of the sky's brightness throughout the observations of HAT-P-20 and TOI-1131 most likely overshadowed the flux reduction expected from the transits [Figure 2] [Figure 4]. This is very plausible as, for instance, the transit depth of TOI-1131 is 0.0043 mag with a brightness of 9.7 mag [20]. Toi-1131's transit depth of only 0.0043 mag is small enough that it could be indistinguishable other random fluctuations in flux across the observational period. HAT-P-20, on the other hand, has a significant transit depth of 0.0204 mag but has a very dim magnitude of 11.34 mag [20]. The HAT-P-20's dimness could explain the missing transit as the star's low brightness could be outweighed by the bright and variable sky, eclipsing any indication of a transit. In contrast, HAT-P-22 has a high brightness of 9.73 mag and a significant depth of 0.0140 mag [20] compared to the two other targets, making its transit more apparent and distinguishable from any random fluctuations in flux caused by the environment or equipment. This leads to the conclusion that the success of a transit observation in these observational conditions is highly dependent on transit characteristics and that chosen target stars should be brighter or as bright as 10 mag with a transit depth over 0.01 mag to successfully record a transit using a similar astronomical setup.

These results concur with those of Hoot [11], Littlefield [16], and Zhang *et al.* [27], conveying that DSLR camera can produce precise and accurate enough photometry to record a exoplanet transit. Just like Littlefield [16] and Zhang *et al.* [27], we were able to observe a transit using a consumer-grade DSLR camera. Our findings show that these conclusions from Hoot [11], Littlefield [16], and Zhang *et al.* [27] extend to urban light-polluted settings like Montreal for bright targets with considerable transit depths. These proof of concept broadens the field of potential astronomical observers, giving amateur and upcoming observers the opportunity to perform significant astronomical photometry with affordable equipment.

It has to be noted that, in all the observations, poor

mount tracking and occasional cloudiness resulted in a considerable portion of the data points having to be discarded as either the target or reference star was not in the field of view, restricting the definiteness of the results. Another factor limiting the certainty of the results is the short time before and after the transit. For further observations, the observation period should span longer before and after the expected transit to have more definite results.

More data points before and after the transit would allow greater analysis on the transit. In this paper, a rudimentary quartic best fit line was used to highlight the transit of HAT-P-22 [Appendix D]. Ideally, for future observations, with more data points outside the transit period, fitting algorithms of transit models such as the Box-Fitting Least Squares model [14] and the Mandel-Agol model [18] could be used. Fitting observed transits using these models would give great insight about the host star and exoplanet's properties: transit duration, stellar radius, and exoplanet radius and density to name a few.

Another significant improvement that could be made for future observations is to incorporate an astronomical driver to the observational setup. An astronomical driver would allow all the equipment (camera, telescope, and mount) to be controlled from a single hub. This would be a considerable step towards observatory amortization. Furthermore, this would allow information such as declination, right ascension, and field size to be embedded in the header of each scientific picture. This improvement would make the data extraction and treatment process significantly faster, allowing for the use of plate solving, alignment, and automatic aperture photometry features in softwares such as *Iris* [3]. This would open the way to make more observations with the possibility of considering many targets and reference stars simultaneously.

In conclusion, the three observations suggest that it is possible to observe a transit in poor observational conditions using a consumer-grade DSLR camera. A target star brighter than around 10 mag with a transit depth over 0.01 mag should be selected to do so. This proof of concept extends the established ability of DSLR cameras to record transits by observing the transit of HAT-P-22 in a light-polluted city like Montreal, creating an affordable entryway to observational astronomy in urban centers and allowing more amateur astronomers to participate in the expansion of exoplanet catalogues.

5 Acknowledgments

I want to express my sincere gratitude to Roger Hajjar, PhD, who has guided me through this research project and my first exposure to the field of astronomy. I also express my gratitude to Nicholas Park, PhD, who encouraged me to undertake this research opportunity and supported me throughout this journey. Finally, I thank the Vanier College Physics Department for providing the necessary equipment making exciting research like this possible.

References

- [1] Exoplanet and Candidate Statistics. *NASA Exoplanet Science Institute*. URL: https://exoplanetarchive.ipac.caltech.edu/docs/counts_detail.html.
- [2] Astropy Collaboration, Adrian M. Price-Whelan, Pey Lian Lim, Nicholas Earl, Nathaniel Starkman, Larry Bradley, David L. Shupe, Aarya A. Patil, Lia Corrales, C. E. Brasseur, Maximilian Nothe, Axel Donath, Erik Tollerud, Brett M. Morris, Adam Ginsburg, Eero Vaher, Benjamin A. Weaver, James Tocknell, William Jamieson, Marten H. van Kerkwijk, Thomas P. Robitaille, Bruce Merry, Matteo Bachetti, H. Moritz Günther, Thomas L. Aldcroft, Jaime A. Alvarado-Montes, Anne M. Archibald, Attila Bodi, Shreyas Bapat, Geert Barentsen, Juanjo Bazan, Manish Biswas, Mederic Boquien, D. J. Burke, Daria Cara, Mihai Cara, Kyle E. Conroy, Simon Conseil, Matthew W. Craig, Robert M. Cross, Kelle L. Cruz, Francesco D'Eugenio, Nadia Dencheva, Hadrien A. R. Devillepoix, J'org P. Dietrich, Arthur Davis Eigenbrot, Thomas Erben, Leonardo Ferreira, Daniel Foreman-Mackey, Ryan Fox, Nabil Freij, Suyog Garg, Robel Geda, Lauren Glattly, Yash Gondhalekar, Karl D. Gordon, David Grant, Perry Greenfield, Austen M. Groener, Steve Guest, Sebastian Gurovich, Rasmus Handberg, Akeem Hart, Zac Hatfield-Dodds, Derek Homeier, Griffin Hosseinzadeh, Tim Jenness, Craig K. Jones, Prajwel Joseph, J. Bryce Kalmbach, Emir Karamehmetoglu, Mikolaj Kaluszynski, Michael S. P. Kelley, Nicholas Kern, Wolfgang E. Kerzendorf, Eric W. Koch, Shankar Kulumani, Antony Lee, Chun Ly, Zhiyuan Ma, Conor MacBride, Jakob M. Maljaars, Demitri Muna, N. A. Murphy, Henrik Norman, Richard O'Steen, Kyle A. Oman, Camilla Pacifci, Sergio Pascual, J. Pascual-Granado, Rohit R. Patil, Gabriel I. Perren, Timothy E. Pickering, Tanuj Rastogi, Benjamin R. Roulston, Daniel F. Ryan, Eli S. Rykoff, Jose Sabater, Parikshit Sakurikar, Jesus Salgado, Aniket Sanghi, Nicholas Saunders, Volodymyr Savchenko, Ludwig Schwardt, Michael Seifert-Eckert, Albert Y. Shih, Anany Shrey Jain, Gyanendra Shukla, Jonathan Sick, Chris Simpson, Sudheesh Singanamalla, Leo P. Singer, Jaladh Singhal, Manodeep Sinha, Brigitta M. SipHocz, Lee R. Spitler, David Stansby, Ole Streicher, Jani Sumak, John D. Swinbank, Dan S. Taranu, Nikita Tewary, Grant R. Tremblay, Miguel de Val-Borro, Samuel J. Van Kooten, Zlatan Vasovic, Shresth Verma, Jose Vinicius de Miranda Cardoso, Peter K. G. Williams, Tom J. Wilson, Benjamin Winkel, W. M. Wood-Vasey, Rui Xue, Peter Yoachim, Chen Zhang, Andrea Zonca, and Astropy Project Contributors. The Astropy Project: Sustaining and Growing a Community-oriented Open-source Project and the Latest Major Release (v5.0) of the Core Package. *apj*, 935(2):167, August 2022. arXiv:2206.14220, doi:10.3847/1538-4357/ac7c74.
- [3] Christian Buil. Iris 5.59, June 2010. URL: <http://www.astrosurf.com/buil/iris-software.html>.
- [4] Environment Canada. Canadian Weather. URL: https://weather.gc.ca/canada_e.html.
- [5] Canon. EOS Utility 3.14.30, January 2022. URL: https://canoncanada.custhelp.com/app/answers/answer_view/a_id/1037800/~eos-utility-3.14.30-for-macos.
- [6] Canon. Digital Photo Professional 4.17.20, March 2023. URL: https://canoncanada.custhelp.com/app/answers/answer_view/a_id/1042544/~digital-photo-professional-4.17.20-for-macos.
- [7] Celestron. Celestron PWI Telescope Control Software 2.4.3, February 2023. URL: <https://www.celestron.com/pages/celestron-pwi-telescope-control-software>.
- [8] Richard Kinne Matthew Templeton Roger Pieri Rebecca Jackson Michael Brewster Mark Blackford Heinz-Bernd Eggenstein Martin Connors Ian Doktor Robert Buchheim Donald Collins Tim Hager Bob Manske Brian Kloppenborg Arne Henden Des Loughney Mike Simonsen Todd Brown Colin Littlefield, Paul Norris and Paul Valleli. TIRIS-Beginner Tutorial. *American Association of Variable Star Observers*. URL: https://www.aavso.org/sites/default/files//IRIS_Beginner_1.pdf.
- [9] Richard Kinne Matthew Templeton Roger Pieri Rebecca Jackson Michael Brewster Mark Blackford Heinz-Bernd Eggenstein Martin Connors Ian Doktor Robert Buchheim Donald

- Collins Tim Hager Bob Manske Brian Kloppenborg Arne Henden Des Loughney Mike Simonsen Todd Brown Colin Littlefield, Paul Norris and Paul Valleli. The AAVSO DSLR Observing Manual. *American Association of Variable Star Observers*, June 2014. URL: https://www.aavso.org/sites/default/files/AAVSO_DSLR_Observing_Manual_v1-2.pdf.
- [10] Charles R Harris, K Jarrod Millman, Stéfan J van der Walt, Ralf Gommers, Pauli Virtanen, David Cournapeau, Eric Wieser, Julian Taylor, Sebastian Berg, Nathaniel J Smith, Robert Kern, Matti Picus, Stephan Hoyer, Marten H van Kerkwijk, Matthew Brett, Allan Haldane, Jaime Fernández del Río, Mark Wiebe, Pearu Peterson, Pierre Gérard-Marchant, Kevin Sheppard, Tyler Reddy, Warren Weckesser, Hameer Abbasi, Christoph Gohlke, and Travis E Oliphant. Array programming with NumPy. *Nature*, 585(7825):357–362, 2020. doi:10.1038/s41586-020-2649-2.
- [11] J. E. Hoot. Photometry With DSLR Cameras. *Society for Astronomical Sciences Annual Symposium*, 26:67, May 2007. URL: <https://ui.adsabs.harvard.edu/abs/2007SASS...26...67H>.
- [12] John D Hunter. Matplotlib: A 2d graphics environment. *Computing in science & engineering*, 9(3):90, 2007.
- [13] Eric Jensen. Tapir: A web interface for transit/eclipse observability. Astrophysics Source Code Library, record ascl:1306.007, June 2013. arXiv:1306.007.
- [14] Geza Kovacs, Shay Zucker, and T. Mazeh. A box-fitting algorithm in the search for periodic transits. *Astronomy and Astrophysics*, 391, 06 2002. doi:10.1051/0004-6361:20020802.
- [15] Eric O. Lebigot. Uncertainties: a Python package for calculations with uncertainties. URL: <https://pythonhosted.org/uncertainties/>.
- [16] C. Littlefield. Observing Exoplanet Transits with Digital SLR Cameras., 38(2):212, December 2010. URL: <https://ui.adsabs.harvard.edu/abs/2010JAVSO..38..212L>.
- [17] David Lorenz. Light Pollution Atlas 2020. 2020. URL: <https://djlorenz.github.io/astronomy/lp2020/>.
- [18] Kaisey Mandel and Eric Agol. Analytic light curves for planetary transit searches. *The Astrophysical Journal*, 580(2):L171–L175, dec 2002. URL: <https://doi.org/10.1086/2F345520>. doi:10.1086/345520.
- [19] Arne Heden Matthew Templeton, Sara Beck and Marl Munkacsy. AAVSO Guide to CCD/CMOS Photometry with Monochrome Cameras. *American Association of Variable Star Observers*, July 2022. URL: https://www.aavso.org/sites/default/files/publications_files/ccd_photometry_guide/CCDPhotometryGuide.pdf.
- [20] Stanislav Poddaný, Luboš Brát, and Ondřej Pejcha. Exoplanet transit database. reduction and processing of the photometric data of exoplanet transits. *New Astronomy*, 15(3):297–301, March 2010. URL: <https://doi.org/10.1016%2Fj.newast.2009.09.001>, doi:10.1016/j.newast.2009.09.001.
- [21] Nikolaus Prusinski. Measuring Linearity, Gain, and Read Noise. June 2017. URL: http://nzp.guru/ref/CCD_paper.pdf.
- [22] Python Core Team. *Python: A dynamic, open source programming language*. Python Software Foundation, 2021. Python version 3.10. URL: <https://www.python.org/>.
- [23] Maik Riechert. rawpy 0.18.0, 2014. URL: <https://letmaik.github.io/rawpy/api/index.html>.
- [24] Ianaré Sévi. ExifRead 3.0.0, May 2022. URL: <https://pypi.org/project/ExifRead/>.
- [25] Pauli Virtanen, Ralf Gommers, Travis E. Oliphant, Matt Haberland, Tyler Reddy, David Cournapeau, Evgeni Burovski, Pearu Peterson, Warren Weckesser, Jonathan Bright, Stéfan J. van der Walt, Matthew Brett, Joshua Wilson, K. Jarrod Millman, Nikolay Mayorov, Andrew R. J. Nelson, Eric Jones, Robert Kern, Eric Larson, C J Carey, İlhan Polat, Yu Feng, Eric W. Moore, Jake VanderPlas, Denis Laxalde, Josef Perktold, Robert Cimrman, Ian Henriksen, E. A. Quintero, Charles R. Harris, Anne M. Archibald, Antônio H. Ribeiro, Fabian Pedregosa, Paul van Mulbregt, and SciPy 1.0 Contributors. SciPy 1.0: Fundamental Algorithms for Scientific Computing in Python. *Nature Methods*, 17:261–272, 2020. doi:10.1038/s41592-019-0686-2.
- [26] M. Wenger, F. Ochsenbein, D. Egret,

- P. Dubois, F. Bonnarel, S. Borde, F. Genova, G. Jasniewicz, S. Laloë, S. Lesteven, and R. Monier. The SIMBAD astronomical database. *Astronomy and Astrophysics Supplement Series*, 143(1):9–22, apr 2000. URL: <https://doi.org/10.1051%2Faas%3A2000332>, doi:10.1051/aas:2000332.
- [27] M. Zhang, G. Á. Bakos, K. Penev, Z. Csubry, J. D. Hartman, W. Bhatti, and M. de Val-Borro. Precision multiband photometry with a dslr camera. *Publications of the Astronomical Society of the Pacific*, 128(961):035001, feb 2016. URL: <https://dx.doi.org/10.1088/1538-3873/128/961/035001>, doi:10.1088/1538-3873/128/961/035001.

A Appendix: Fields of View

These figures are the fields of view of HAT-P-20, HAT-P-22, and TOI-1131 along with their comparison stars during the nights of observations.



Figure 7: Field of View of Target [HAT-P-20](#) and Reference [TYC 1914-551-1](#) on March 19th, 2023



Figure 8: Field of View of Target [HAT-P-22](#) and Reference [HD 233728](#) on April 2nd, 2023

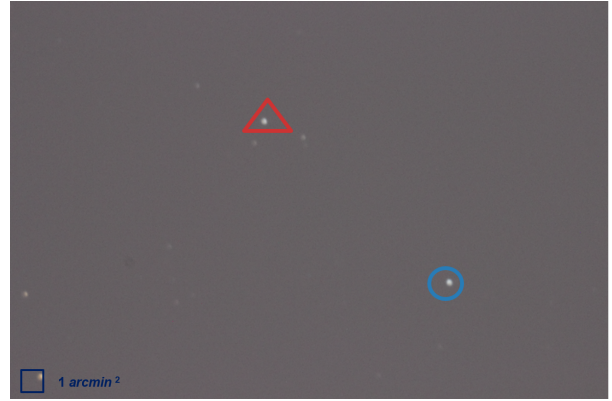


Figure 9: Field of View of Target [TOI-1131](#) and Reference [TYC 4190-97-1](#) on April 15th, 2023

B Appendix: CR2 to FIT Conversion

This code was used to sum the three channels of RAW CR2 files and convert it to FIT files while conserving the native headers of the observation of HAT-P-22.

```
from astropy.io import fits
import rawpy, os, re, exifread, numpy as np

def tofits(initialPath, finalPath):
    for i, val in initialPath.items():
        for d in os.listdir(val):
            if d.endswith('.CR2'):
                f = os.path.join(val, d)
                print(f)
                with open(f, 'rb') as file:
                    h = exifread.process_file(file,
                                              details=False, stop_tag='UNDEF')
                new_dic = {}
                for key, value in h.items():
                    key = re.sub(r'[a-zA-Z0-9-_]', '',
                                key)
                    new_dic[key] = str(value)
                data_head = new_dic

                with rawpy.imread(f) as raw:
                    image = raw.raw_image_visible.copy()
                if len(image.shape) == 3:
                    image = np.sum(image, axis=2)

                hdu = fits.PrimaryHDU(image)
                fits_f = os.path.join(finalPath[i], d,
                                     replace('.CR2', '.fit'))
                hdu.writeto(fits_f, overwrite=True)

                with fits.open(fits_f, mode='update'):
                    as_hdulist:
                    header = hdulist[0].header
                    header.update(data_head)
                    hdulist.flush()
```

C Appendix: Data Analysis

This code was used to extract, process, and plot the data from an *Iris* output text file.

```
import matplotlib.pyplot as plt
from uncertainties import ufloat
from uncertainties.umath import *
import math as mt
import numpy as np
import os
```

```

import exifread

def readData(dataPath, starName, miss):
    lst = []
    with open(os.path.join(datapath, starName), 'r') as f:
        for line in f:
            if 'Pixel_number_in_the_inner_circle' in line:
                pixelnum = float(line.split('=')[1].strip())
            elif 'Intensity' in line:
                intensity = float(line.split('=')[1].split('_')[0].strip())
                magnitude = float(line.split('_')[2].replace('-', '').strip())
            elif 'Background_mean_level' in line:
                background = float(line.split('=')[1].strip())
                lst.append([intensity, magnitude, background * pixelNum])
    newLst = []
    ind = 0
    for i in range(len(lst) + len(miss)):
        if i + 1 in miss:
            newLst.append([mt.nan, mt.nan, mt.nan])
        else:
            newLst.append(lst[ind])
            ind += 1
    return newLst

def extractTime(imgPath):
    with open(imgPath, 'rb') as f:
        data = exifread.process_file(f, details=False,
                                      stop_tag='UNDEF')
    lst = str(data['Image_DateTime']).split('_')[1].split(':')
    return [int(lst[0]) * 3600 + int(lst[1]) * 60 + int(lst[2]),
            str(data['Image_DateTime'])]

def dataArray(dataPath, starName, miss):
    lst = readData(dataPath, starName, miss)
    arr = []
    for i, val in enumerate(lst):
        arr.append(ufloat(val[0] - val[2], np.sqrt(val[0] - val[2])))
    return arr

def analysis(dataPath, cr2Path, targetName,
            comparisonName, targetMiss, ComparisonMiss):
    y = dataArray(dataPath, targetName, targetMiss)
    t = dataArray(dataPath, comparisonName, ComparisonMiss)

    x0 = 0
    difference24h = 0
    date = '0'
    for i, val in enumerate(os.listdir(cr2Path)):
        imgPath = os.path.join(cr2Path, val)
        time = extractTime(imgPath)
        if i == 0:
            x0 = time[0]
            date = time[1]
            difference24h = 24 * 3600 - x0
        if u < 0:
            u = (time[0] + difference24h) / 60
        x.append(u)

    y = np.divide(y, t)
    y = np.divide(y, np.nanmedian(y))
    yval = []
    ysig = []
    for i in y:
        yval.append(i.n)
        ysig.append(i.s)

    plt.scatter(x, yval, s=3)
    plt.errorbar(x, yval, yerr=ysig, fmt="none",
                 capsizes=3)
    plt.title(f'Relative_Normalized_Flux_of_{targetName}_on_{comparisonName}')
    plt.xlabel(f'Time_Elapsed_since_{date}-(min)')
    plt.ylabel('Relative_Normalized_Flux')
    plt.show()

```

D Appendix: Transit Curve Fitting

This code was used to combine points (5 and 3-point average) and best-fit a quartic curve to outline the transit of HAT-P-22 [Figure 6] [Figure 10].

```

import scipy.optimize as opt
import numpy as np

```

```

import matplotlib.pyplot as plt

def qua(x, a, b, c, d, e):
    return a*x**4 + b*x**3 + c*x**2 + d*x + e

def qua_model(timeArr, fluxArr, fluxErr):
    popt, pcov = opt.curve_fit(qua, timeArr, fluxArr,
                               sigma=fluxErr, absolute_sigma=True)

    timeCurve = np.linspace(0, timeArr[-1], 200)
    fluxCurve = qua_model(timeCurve, popt[0], popt[1],
                          popt[2], popt[3], popt[4])

    return [timeCurve, fluxCurve]

def transit_avg_curve(timeArr, fluxArr, fluxErr, div,
                      formattedInitialTime):
    timeAvg = []
    fluxAvg = []
    fluxSigAvg = []

    for i in range(np.floor(len(fluxArr)/div)):
        timeAvg.append(np.nanmean(timeArr[div*i:div*i+div]))
        fluxAvg.append(np.nanmean(fluxArr[div*i:div*i+div]))
        fluxSigAvg.append(np.sqrt(np.nanmean(np.array(
            fluxErr[div*i:div*i+div])**2)))

    quaLine = qua_model(timeAvg, fluxAvg, fluxSigAvg)

    plt.plot(quaLine[0], quaLine[1], c='red')
    plt.scatter(timeAvg, fluxAvg, s=3, label='HAT-P-22')
    plt.errorbar(timeAvg, fluxAvg, yerr=fluxSigAvg, fmt="none",
                 capsizes=3)
    plt.xlabel(f'Time_Elapsed_since_{formattedInitialTime}-(min)')
    plt.ylabel('Relative_Normalized_Flux')
    plt.show()

```

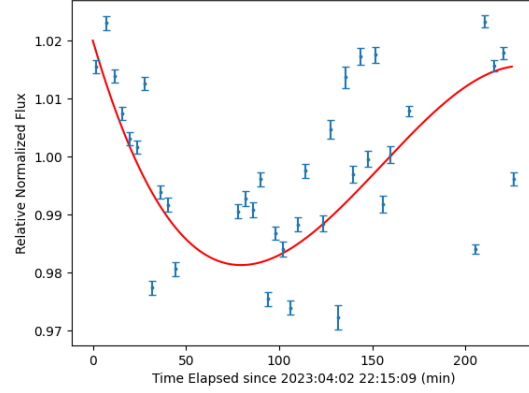


Figure 10: Relative Normalized Flux of HAT-P-22 on HD 233728 on April 2nd, 2023 from 22h15 until 01h59 EDT, with Combined Data Points (a 3-Point Average) and Transit Outline